Supramolecular host-guest chemistry for applications in theranostics

Spa, S.J.

CHAPTER 5

Orthogonal Functionalization of Ferritin via Supramolecular Re-Assembly

ABSTRACT

To investigate if the degree of functionalization of ferritin could be controlled using a supramolecular self-assembly process, two photophysical separable batches of ferritin were created by functionalizing ferritin capsids with either Cy3- or Cy5-dye (loading rate of about 50%). After dis-assembly, Cy3-, Cy5- as well as non-functionalized ferritin subunits were mixed in variable ratios. Photophysical measurements revealed that the ratio in which the subunits were mixed was indeed indicative for the ratios in which the functionalized subunits were observed in the re-assembled capsids. During re-assembly, however, a slight preference for the inclusion of non-functionalized subunits was observed, indicating that the reactivity decreased following functionalization. The iron biomineralization properties of ferritin were retained by the multi-functionalized capsids as Fe^{II} diffused rapidly inside, making it visible by transmission electron microscopy (TEM). These combined data indicate that it is possible to functionalize ferritin in an orthogonal manner using the supramolecular interaction between ferritin subunits.

INTRODUCTION

In nature, supramolecular protein assemblies can provide functional structures, which in fact can be seen as natural (bio-)nanoparticles. Examples are: viral capsids,[1,2] bacteriophages,[3] and ferritin.[4] While the first two are disease related, the latter is responsible for a critical component in live, namely the iron metabolism of cells.[5,6] Through chemical manipulation, however, ferritin can also be applied for other purposes. Promising ferritin based drug carriers, for example for photodynamic therapy,[4,7] have been developed by replacing the iron core with (small) drug molecules.[8-10] The relatively large surface area of ferritin also allows for a high loading capacity of fluorescent dyes and/or targeting ligands.[11-13] However, among the many ferritin derivatives developed, the MRI contrast agents seem to be the most promising.[11,14] These agents, although functionalized, retain the natural iron mineralization property of ferritin. After mineralization, iron is present in the 8 nm cavity of ferritin capsids as ferrihydrite, and provides contrast on MRI.[15-17]

Large non-covalent natural complexes such as DNA helices, viruses and organelles, assemble into complex structures in an controlled manner.[18,19] By copying from nature, the control on the composition in polymer cross-linking was improved via orthogonal multi-site self-assembly, obtaining polymers with tunable functionality.[20-22] In a similar approach, orthogonally functionalized nanofibers were created by the multicomponent co-assembly of integrin binding ligands Gly-Arg-Gly-Asp-Ser (GRGDS), Pro-His-Ser-Arg-Asn (PHSRN), and fluorophore functionalized building blocks.[23] Furthermore, it has been shown that dual functionality on spherical protein capsids, like cowpea chlorotic mottle virus, could be obtained by re-assembly of two differently functionalized protein subunits.[24-26]

The surface of (bio-)nanoparticles, like ferritin, can be modified by conventional conjugation procedures targeting the amino acids such as lysine.[2,27] Although a substantial collection of bio-conjugation techniques are available, controlled introduction of multiple functionalities via this route remains challenging.[28] We reasoned that an orthogonal functionalization approach via consecutive dis- and re-assembly could provide the opportunity to control the degree of (multi)functionality on ferritin scaffolds. Ferritin, a bio-nanoparticle consisting of 24 identical protein subunits each 20 kDa in weight on average,[29] can be dis- and re-assembled by alteration of the pH.[30,31] To investigate if three different types of subunits could be introduced controllably via supramolecular re-assembly, we functionalized (apo)ferritin with either Cy3 or Cy5, while retaining some non-functionalized subunits (Figure 1, A). Different subunits were then mixed in three

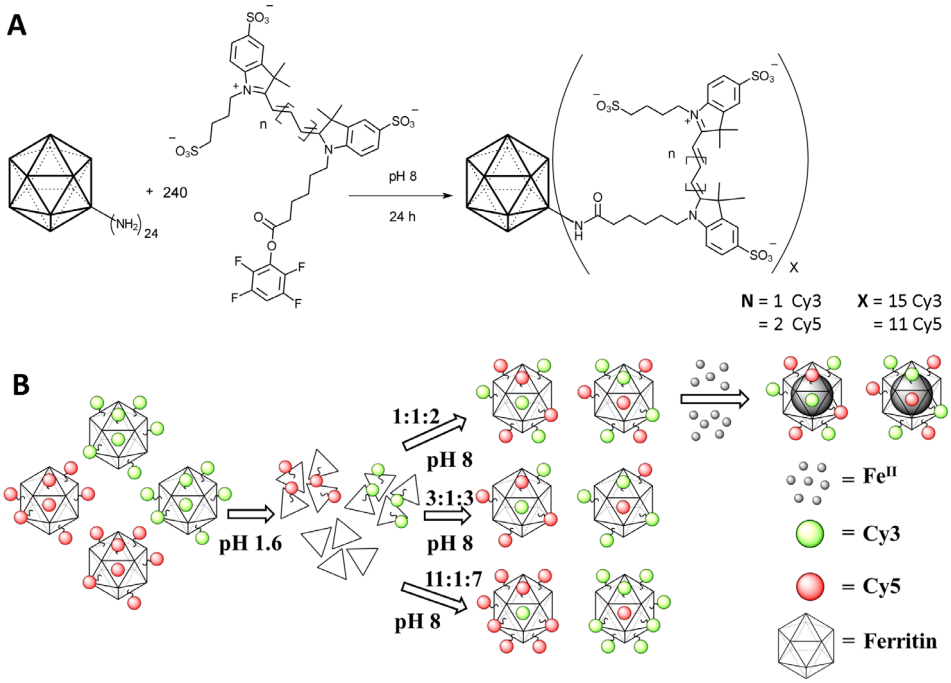

Figure 1. **A**) Functionalization of ferritin with a Cy3 or Cy5 dye, 10 eq. to ferritin subunit, in phosphate buffer pH 8. **B**) Orthogonal functionalization of ferritin with Cy3 (green) and Cy5 (red). Cy3-, Cy5-, and non-functionalized subunits are added together in the indicated ratio, following re-assembly at pH 8. After re-assembly functionalized capsids are mixed with Fe^{II} (grey) to obtain iron loaded ferritin capsids.

different ratios (Figure 1, B) and after re-assembly we evaluated how the ratio of these statistical mixtures influenced the functionalization of newly formed capsids. The photophysical interaction between the two dyes enabled accurate analysis of the orthogonal functionalization. After re-assembly, the multi functionalized ferritin capsids were exposed to Fe^{II}-ions to evaluate if they retained their intrinsic iron biomineralization properties (Figure 1, B).

EXPERIMENTAL

General

Solvents and chemicals were obtained from Actu-All (Oss, The Netherlands) and Sigma Aldrich (Zwijndrecht, The Nether-lands), were used without further purifications. The

apoferritin from equine spleen was obtained from Sigma Aldrich and was stored in aliquots (50 µL, 37 µg/µL in PBS) at 4 °C. Short before the experiments, sufficient aliquots of apoferritin were washed 3 times with phosphate buffered saline (PBS) over a 100 kDa to re-move free subunits and small contaminants. Other ferritin fil-trations were also performed with Amicon Ultra-0.5 mL Centrifu-gal Filters from Merck Millipore (Amsterdam, The Netherlands). Ferritin concentrations were determined by absorption measurements (280 nm, ε-subunits = 14565 L mol^{-1} cm^{-1}) with a Nanodrop ND-1000 spectrophotometer from thermo scientific (Landsmeer, The Netherlands), just as the other UV/Vis absorption measure-ments. SEC was performed on an Aktatm Pure 25 instrument from GE Healthcare (Eindhoven, The Netherlands), if sample collection was required the corresponding fraction collector F9-R was de-ployed. The size exclusion column was a superdex 200 (GE Healthcare), and SEC was performed with 600 µL injection volume with PBS as eluent. The PBS was obtained from B. Braun (Oss, The Netherlands) in sterile and oxygen free conditions and was applied without further treatment. The fluorescence measurements were performed on a LS55 fluorescence spectrometer from Perkin–Elmer (Groningen, The Netherlands). NMR spectra were mea-sured on Bruker DPX 300 Hz (Leiderdorp, The Netherlands). Mass spectra were measured on a Bruker microflex MALDI-TOF. TEM imaging was performed on a FEI Tecnai 12 BioTwin 120 kV TEM (Eindhoven, The Netherlands). ICP-MS measurements were performed on a Thermo Finnigan Element 2 equipped with an autosampler and a conical glass concentric from thermo scientific (Landsmeer, The Netherlands). For HPLC analysis and purifica-tions a Waters HPLC system (Etten-Leur, The Netherlands) con-sisting of HPLC 1525 Pump and 2489 UV/Vis detector using a Reprosil-Pur 120 C18-AQ 10 µm column (250 20 mm) for purifi-cation and a Reprosil-Pur C18-AQ 5 µm column (250 4.6 mm) for analysis, from Dr. Maisch (Ammerbuch, Deutchland).

Synthesis of Cy5$(SO_3)_2$-SO_3–CO_2H and Cy3$(SO_3)_2$-SO_3–CO_2H

Both Cy5 [Cy5$(SO_3)_2$-SO_3–CO_2H] and Cy3 [Cy3$(SO_3)_2$-SO_3–CO_2H] were synthesized according to literature procedure.[32]

Synthesis of Cy5-TFP (Figure 1, A)

Cy5$(SO_3)_2$-SO_3–CO_2H (190 mg, 0.25 mmol) was dissolved in DMF (10 mL). To this DCC (77 mg, 0.37 mmol) and TFP (125 mg, 0.75 mmol) was added and the reaction was stirred overnight at room temp. The next day an-other equivalent of DCC and TFP were added, together with N,N-diisopropylethylamine (DIPEA, 124 µL, 0.75 mmol). The day here-after, the reaction mixture was added to 250 mL of EtOAc and a blue precipitate was isolated.

The crude product was first purified by silica column chromatography (40% MeOH in EtOAc) and fur-ther purified by reversed phase HPLC with a gradient from 5% MeCN to 95% MeCN in H2O (containing 0.1% TFA) in 100 min. Pure fractions were pooled and lyophilized, which yielded 55 mg (24%) of pure product. ^{1}H NMR [300 MHz, $(CD_3)_2SO$, 25 °C]: δ = 8.35 (t, J = 13.1 Hz, 2 H, CH of bridge), 7.93 (m, 1 H, CH of TFP), 7.80 (s, 2 H, Ar-H), 7.62 (d, J = 8.2 Hz, 2 H, Ar-H), 7.33 (dd, J = 16.6, 8.3 Hz, 2 H, Ar-H), 6.58 (m, 1 H, CH of bridge), 6.36 (m, 2 H, CH of bridge), 4.07 (m, 4 H, N-CH2), 2.79 (t, J = 7.1 Hz, 2 H, CH2COOC), 2.55 (m, 2 H, CH2-SO3), 1.97–0.93 [m, 22 H, $5CH_2$ with s at 1.68 for C-$(CH_3)_2$] ppm. ^{13}C NMR [75 MHz,$(CD_3)_2SO$, 25 °C]: δ = 174.33, 169.51, 154.36, 154.06, 145.28, 145.13, 142.03, 141.89, 140.57, 140.48, 126.04, 119.89, 110.30, 110.06, 104.44, 103.69, 103.35, 101.27, 95.37, 54.93, 50.58, 49.46, 48.91, 33.46, 27.07, 26.66, 25.84, 25.61, 24.20, 22.37 ppm. MS (MALDI-TOF): $[M]^+$ calculated for $C_{41}H_{45}F_4N_2O_{11}S_3^+$: 913.2, found 913.6 ppm.

Synthesis of Cy3-TFP (Figure 1, A)

Cy3$(SO_3)_2$-SO_3 (111 mg, 0.15 mmol) was dissolved in DMF (10 mL). To this DCC (62 mg, 0.30 mmol), tetrafluorophenol (TFP, 100 mg, 0.60 mmol), and DIPEA (100 µL, 0.6 mmol) was added and the reaction was stirred overnight at RT. The next day another equivalent of DCC, two equivalents of TFP and 2 equiv. of DIPEA were added and reacted over weekend. The reaction was concentrated in vacuo and purified by silica column chromatography (40% MeOH in EtOAc). The resulting product was lyophilized, which yielded 44 mg (31%) of pure product. ^{1}H NMR [300 MHz, $(CD_3)_2SO$, 25 °C]: δ = 8.36 (t, J = 13.4 Hz, 1 H, CH of bridge), 7.92 (m, 1 H, CH of TFP), 7.79 (s, 2 H, Ar-H), 7.66 (d, J = 8.2 Hz, 2 H, Ar-H), 7.42 (dd, J = 14.2, 8.4 Hz, 2 H, Ar-H), 6.57 (dd, J = 13.4, 3.2 Hz, 2 H, CH of bridge), 4.13 (m, 4 H, N-CH2), 2.82 (t, J = 7.1 Hz, 2 H, CH2COOC), 2.51 (m, 2 H, CH2-SO3), 1.87–0.94 [m, 22 H, 5CH2 with s at 1.70 for C-$(CH_3)_2$] ppm. ^{13}C NMR [75 MHz, $(CD_3)_2SO$, 25 °C]: δ = 174.14, 169.58, 149.94, 145.78, 145.73, 141.87, 141.75, 140.10, 126.24, 119.86, 119.82, 110.86, 110.67, 104.75, 104.43, 104.12, 103.10, 50.67, 48.91, 43.90, 43.77, 32.35, 27.42, 26.71, 26.04, 25.29, 24.04, 22.54 ppm. MS (MALDI-TOF): $[M]^+$ calculated for $C_{39}H_{43}F_4N_2O_{11}S_3^+$: 887.2, found 887.8.

Ferritin Functionalization with Cy3 or Cy5

Filtered apoferritin (5 mg, 245 pmol) in PBS (300 µL) was mixed with phosphate buffer (300 µL, pH 8, 0.1 M) and subsequently a solution of Cy5-TFP (2 mg, 2.19 µmol) or Cy3-TFP (2 mg, 2.25 µmol) in DMSO (10 µL) was added. After one night stirring at RT the ferritin capsids were washed by sequential filtering over 100 kD Amicon filters until the filtrate was no longer blue. By absorption measurements the concentration of Cy3 ($\varepsilon = 150 \cdot 10^3$

L mol^{-1} cm^{-1}) or Cy5 (ε = $250 \cdot 10^3$ L mol^{-1} cm^{-1}) and ferritin subunits (ε = $14.6 \cdot 10^3$ L mol^{-1} cm^{-1}) was determined. The reaction was performed three times with the same batch of apoferritin to obtain a final labelling ratio of 0.65 Cy3/subunit and 0.47 Cy5/subunit, corresponding with 15 Cy3/ferritin and 11 Cy5/ferritin respectively.

Dis-Assembly and Re-Assembly of Ferritin

Method 1: Conventional method at room temp and *Method 2*: Conventional method at 37 °C. To apoferritin (50 µL, 1.85 mg) in H_2O (3 mL), HCl solution (195 µL, pH 0.3, 0.5 M) was added to obtain a pH of 1.6. After 15 min of stirring at RT an aliquot (200 µL) was taken and diluted to 600 µL for SEC analysis. Simultaneously, NaOH solution (205 µL, pH 13.7, 0.5 M) was added drop wise to the reaction mixture returning it slowly to physiological pH. Subsequently, the reaction was stirred for at least 24 h at RT (method 1) or 37 °C (method 2). Re-assembled capsids were obtained with 14 ± 13% yield (method 1) and 15 ± 11% yield (method 2).

Method 3: Change of pH by buffer replacement via filtration.
Washed apoferritin (20 µL, 0.36 mg) was added to HCl-KCl buffer (200 µL, pH 1.6, 0.1 M, 0.05 % w/w Tween 20), resulting in a concentration of 1.6 mg/mL ferritin. The reaction mixture was shaken at RT for 15 min and the volume was subsequently reduced to 100 µL by filtration through 10 kDa Amicon filter. Sodium phosphate buffer (400 µL, pH 8.6, 0.1 M, 0.05 % w/w Tween 20) was added, followed again by reducing the volume to 100 µL. This was repeated three times, thereby replacing the HCl-KCl buffer step by step. The reaction mixture was recovered from the filter and supplemented with sodium phosphate buffer (500 µL, pH 8.6, 0.1 M, 0.05 % w/w Tween 20) obtaining a final pH of 8.6. The resulting ferritin solution (600 µL, 0.62 mg/mL, pH 8.6) was shaken at 37 °C for at least 24 h. Re-assembled capsids were obtained with 14 ± 9% yield.

Method 4: Change of pH by adding a basic buffer to an acidic solution.
Washed apoferritin (20 µL, 0.36 mg) was added to HCl-KCl buffer (200 µL, pH 1.6, 0.03 M, 0.05 % w/w Tween 20), resulting in a concentration of 1.6 mg/mL ferritin. The reaction mixture was shaken at room temperature for 15 min and subsequently, sodium phosphate buffer (400 µL, pH 8.6, 0.05 M, 0.05 % w/w Tween 20) was added, bringing the pH towards 8. The resulting ferritin solution (600 µL, 0.62 mg/mL, pH 8) was shaken at 37 °C for at least 24 h. Re-assembled capsids were obtained with 25 ± 5% yield.

Orthogonal Functionalization of Ferritin with Cy-Dye According to Method 4

Cy3-ferritin subunits, Cy5-ferritin subunits and unmodified ferritin subunits were varied in the ratios of 4.5:4.5:13 (experiment A), 10.7:3.5:9.8 (experiment B), and 13.8:1.3:12.7 (experiment C) on average. Experiment A was performed twice, B was performed three times and C was performed five times. For each experiment a separate stock solution of dis-assembled Cy3- and Cy5-ferritin capsids was prepared. First, the necessary quantities of Cy3- and Cy5-ferritin capsids for each reaction were calculated via:

$$Cy3 = \frac{0.66 \cdot 10^{-9}}{\left(\frac{0.65}{0.47N} + 1\right)} \qquad Cy5 = \frac{0.66 \cdot 10^{-9}}{\left(\frac{0.47N}{0.65} + 1\right)}$$

with Cy3 or Cy5 = mol Cy3- or Cy5 functionalized ferritin capsids, N = the ratio of Cy3-subunit/Cy5-subunits aimed at, $0.66 \cdot 10^{-9}$ the total quantity (mol) of ferritin capsids in each separate reaction, and 0.65 or 0.47 being the labelling yields of the Cy-dye functionalized ferritin. Secondly, the quantities of Cy3-ferritin capsids (0.56 nm, 1.36 nm, 2.96 nm) and Cy5-ferritin capsids (0.77 nmol, 0.63 nmol, or 0.37 nmol), calculated for two or more experiments of A, B, or C, were dissolved in separate solutions of HCl-KCl buffer (200 µL, 300 µL or 500 µL, respectively), resulting in the stock solutions consisting of Cy3- and non-functionalized subunits, or Cy5- and non-functionalized subunits. For each re-assembly reaction, aliquots (100 µL) of the appropriate stock solutions were mixed together (1:1, 200 µL final volume) to obtain mixtures of dis-assembled Cy3-, Cy5- and non-functionalized ferritin subunits in the ratios aimed at. Then, the sodium phosphate buffer (400 µL) was added and the reaction shaken for 24 h at 37 °C. Both reactions of experiment A were pooled and concentrated to 600 µL using a 100 kDa Amicon filter. The concentrated sample was purified by SEC and the fractions from 10 to 12 mL and from 13 to 15.5 mL elution volume (0.5 mL/fraction) collected. The same was done for experiment B and C. The obtained re-assembled ferritin capsids were further analysed by TEM, absorption and fluorescence spectroscopy (Figures 2 and 3). The orthogonally functionalized ferritin capsids were obtained with approximately 17 ± 2% yield in all three reactions.

Yield Calculations of Re-Assembly

The yield of the re-assembly method was computed from the SEC data. The total area under the SEC curve was equated to 100%, hereby the sum of area underneath the peak of interest is the yield of the corresponding construct. To determine the percentage of the re-assembled ferritin capsids in the sample, the area under the peak at retention volumes 13–15.5 mL (re-assembled capsids) where used (Figure 2, B).

Iron Incorporation

The incorporation of iron was performed following a literature procedure with small modifications.[33] In short, apoferritin (non-functionalized, Cy3-functionalized, and Cy3-, Cy5 functionalized by re-assembly) was dissolved in tris buffer (pH 8, 50 mM Tris-HCl, 100 mM NaCl, 10 mm $MgCl_2$) to obtain a 0.5 µM ferritin capsid concentration. Subsequently 1000 X excess to ferritin capsids of $(NH_4)_2Fe(SO_4)_2$ dissolved in degassed Milli-Q (< 0.6 mg/mL), was slowly added in 10 steps. After 30 min standing exposed to air, the capsids were washed 3 times with demi water over a 100 kDa Amicon filter and subsequently collected in tris-buffer (100 µL final volume).

TEM Protocol

For TEM imaging 5 µL PBS containing approximately $2.5 \cdot 10^{14}$ ferritin capsids was incubated on carbon and formvar coated cupper EM grids for 1 min, and subsequently the sample was stained with one drop of uranyl acetate 2% for 10 seconds. After each step the remaining solvent was removed by blotting.

ICP-MS Protocol

An analytical sample was digested in a per-fluoroalkoxy (PFA) microwave digestion tube to which 10 mL of nitric acid (70 % HNO3) were added. All samples were digested in a MARS microwave system for 50 min. The temperature program was as follows: at 1200 W power from 20 to 150 °C in 15 min, then to 180 °C in 15 min, and finally constant at 180 °C for 20 min. Fol-lowing digestion and cooling to room temperature the digest was diluted and analyzed with a Thermo Finnigan Element 2 equipped with an auto sampler and a conical glass concentric nebulizer, and operated at an RF power of 1000 W. The argon gas flows were at the following settings; plasma, 15 L/min; nebulizer, 1.1 L/min; auxiliary, 1.2 L/min. The sample flow rate to the nebulizer was set at 0.5 mL/min. To minimize polyatomic interferences from 36Ar16O, the instrument was operated in medium resolution mode and iron was measured at m/z 55.85.

RESULTS AND DISCUSSION

Re-Assembly of Ferritin Capsids

The heteropolymeric apoferritin from equine spleen was selected for the investigation, since it is one of the commonly applied and more investigated ferritin platforms.[31, 34-37]

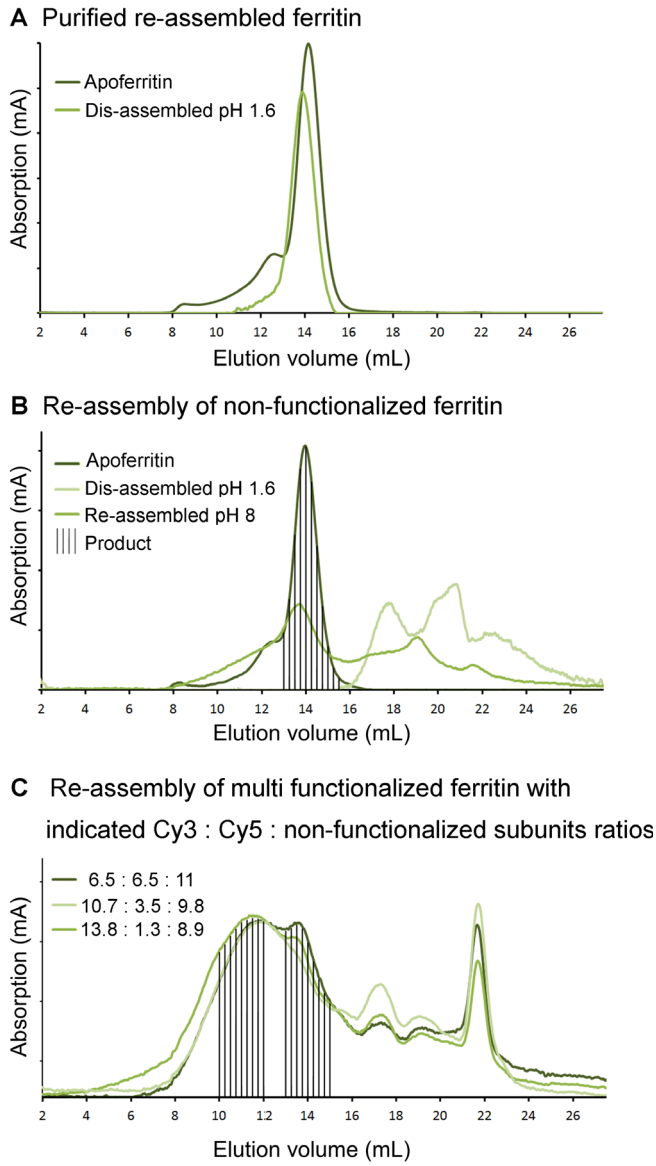

Figure 2. Size exclusion chromatography curves **A**) Ferritin capsids before re-assembly and after dis- and re-assembly following purification. **B**) SEC curves of apoferritin, dis-assembled subunits (pH 1.6), and after re-assembly (pH 8). The fraction containing correctly sized capsids is highlighted. **C**) Crude reaction sample after orthogonal functionalization of ferritin via re-assembly, with indicated ratios of Cy3:Cy5:non-functionalized subunits. Fraction containing aggregates (10–12 mL) and correctly formed capsids (13–15.5 mL) are highlighted. The corresponding TEM images revealing the composition of the SEC fractions are given in Figure 3 (D and C), respectively.

However, in our hands the literature procedure for the re-assembly of ferritin capsids[30,31] proved to be cumbersome and gave a low reproducibility. To improve the reproducibility and ease of the assembly process, we set-up an alternative re-assembly protocol. From four methods tested (see Experimental section), the one by which we achieved the best pH control and smallest yield variation was considered best (method 4). In this method dis-assembly was realized by dissolving ferritin in a hydrochloric acid solution of pH 1.6. Subsequent re-assembly was accomplished by adding a weak phosphate buffer of pH 8.6 (twice the volume of the acidic solution). The resulting basic solution had to be shaken for two days (37 °C) to reach equilibrium.

Re-assembled ferritin capsids were analysed and purified by size exclusion chromatography (SEC). The peaks corresponding to the parental ferritin capsids and (purified) re-assembled ferritin capsids both eluted from the column after the same amount of elution volume (Figure 2, A), indicating both compounds were identical in size. For further confirmation both structures were analysed by transmission electron microscopy (TEM). The parental ferritin capsids could be imaged as circular structures of 12.1 X 0.7 nm in diameter using negative staining (Figure 3, A). These observations confirm previous reports.[38] After re-assembly and purification the TEM images revealed comparable circular structures with a diameter of 12.6 X 0.7 nm, indicating the re-assembly method was successful (Figure 3, B–C).

In the literature, re-assembly of ferritin is referred to as a simple and robust method;[36,39] the yield of this reaction is seldom mentioned and successful re-assembly is often not verified. However, there are reports of low yielding ferritin re-assemblies.[40-41] We also obtained a relatively low re-assembly yield for non-functionalized ferritin (25 ± 5%). It is proposed that subunits re-assemble through the formation of (stable) dimers, trimers and dodecamers.[42] Hereby, the reaction steps; $24M_1 \leftrightarrow 8M_2 + 8M_1 \leftrightarrow 8M_3 \leftrightarrow 4M_6 \leftrightarrow 2M_{12} \leftrightarrow 1M_{24}$ are proposed (with M_1 referring to a single subunit).[40-42] Formation of other intermediate assemblies is thought to result in so-called "dead-end structures",[29] such as the rod-like structures with random dimensions that we found as side products (Figure 3, D). According to Kim et al. these structures may originate from the trimer intermediate.[41]

After investigating the structure of ferritin capsids by small-angle X-ray scattering (SAXS), Kim et al.[41] concluded that re-assembly of ferritin is only pseudo reversible over a pH range of 2.66 to 10, and that a pH < 2 is necessary for complete dissociation. The same group also stated that from pH < 2 intact ferritin capsids could never be fully recovered; one or two subunits would always be missing after re-assembly. We, however, have not found any indications suggesting the re-assembled capsids miss a subunit. In fact TEM analysis

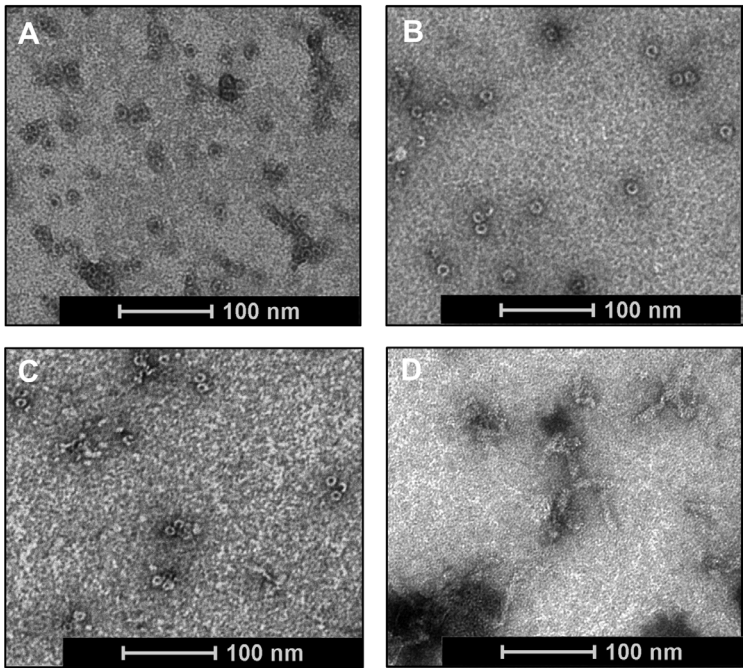

Figure 3. TEM images of ferritin capsids, stained with uranyl acetate. **A**) Parental ferritin capsids. **B**) Re-assembled ferritin capsids. **C**) SEC fraction containing re-assembled multi functionalized ferritin capsids. **D**) SEC fraction containing aggregates.

indicated closed-ring structures. This said we also lack proof that the re-assembled capsids comprise of 24 subunits.

Conjugation of Cy3 or Cy5 to Ferritin

To create two chemically similar but photophysically separable batches of ferritin capsids, one batch of ferritin was functionalized with Cy3- and another with Cy5-dye (Figure 1, A). For efficient conjugation the Cy-dyes were activated as tetrafluorophenol (TFP) esters. The TFP ester proved to be less prone to hydrolysis than the more generally applied N-hydroxylsuccinimide (NHS) ester and as a result higher labelling yields were obtained compared to NHS activated Cy-dyes (data not shown). After functionalization, labelling yields of 15 (62.5 %) Cy3 or 11 (45.8 %) Cy5 dyes on each ferritin capsid were obtained. The labelling yields were derived from the ratio between the subunit- and Cy-dye concentration, calculated from the absorption spectra measured at 280 nm (Cy3) and 550 nm (Cy3) or 650 nm (Cy5).

Table 1. Ratios of Cy3-, Cy5- and non-functionalized subunits.

Dis-assembled subunits Cy3 : Cy5 : non-functionalized	Re-assembled capsids Cy3 : Cy5 : non-functionalized
6.5 : 6.5 : 11	4.4 : 4.1 : 15.5
10.7 : 3.5 : 9.8	8.1 : 3.4 : 12.5
13.8 : 1.3 : 8.9	9.0 : 1.3 : 13.7
0.0 : 11.3 : 12.7	0.0 : 9.8 : 14.2
15.6 : 0.0 : 8.4	14 : 0.0 : 10.0

Orthogonal Functionalization with Cy3 and Cy5 by Supramolecular Re-Assembly

To investigate if the degree of functionalization could be controlled using supramolecular self-assembly processes, the two separately functionalized batches of ferritin were dis-assembled and mixed. By mixing Cy3-functionalized, Cy5-functionalized and non-functionalized subunits at pH 1.6 in variable ratio's following re-assembly at pH 8 (Table 1), we evaluated how the ratio of this mixture influenced the orthogonal functionalization of newly formed capsids. To obtain the desired Cy-dye functionalized sub-units ratios (Table 1), the number of Cy3-functionalized subunits was increased, while the number of Cy5-function-alized subunits was decreased; Cy5 was detectable at a lower concentration range than Cy3, and therefore more suitable for use at lower quantities (Figure 4, A).

Different to what we observed after the re-assembly of non-functionalized ferritin subunits, re-assembly using differently functionalized subunits merely yielded a small (shoulder) peak of product, while the peak belonging to the aggregates increased substantially (Figure 2, C). Although less pronounced, an increase in aggregate formation was also observed after the individual re-assembly of Cy3- or Cy5-functionalized ferritin capsids (data not shown). TEM analysis revealed that correctly formed capsids were still the main content in the 13–15.5 mL elution volume fractions (Figure 3, C) and the same analysis indicated that these samples contained ≤ 10 % pollution of larger constructs. The samples at elution volume 10–12 mL consisted of larger aggregates of which some adopted a rod like conformation with 5 X 40 nm dimensions (Figure 3, D).

The degree of functionalization was derived from the absorption spectra (Figure 4, A), assuming the re-assembled capsids were build up from 24 subunits. Ratio's calculated for capsids consisting of 23 subunits did not result in significant different values (less than 1 % variation). Table 1 reveals that the ratios in which Cy3-functionalized, Cy5-func-tionalized, and non-functionalized subunits were mixed was indicative for the ratios in which they were observed on the re-assembled ferritin capsids. However, we did observe small

deviations between the Cy3- and Cy5-ratios when adding the variable subunits in the maximum ratio of 13.8:1.3:8.9. When differently functionalized subunits where mixed, in all cases the relative ratio of non-functionalized subunits increased slightly. This trend was less pronounced when the re-assembly was performed with only one type of Cy-dye functionalized subunit.

Although our experiments indicate that the envisioned orthogonal functionalization with three functionalities via ferritin self-assembly is feasible, the presence of relatively small Cy-dyes on a protein subunit already seems to negatively influence the delicate re-assembly process (Figure 2, C). Moreover, the supramolecular re-assembly process of non-functionalized ferritin subunits seems to have a higher reactivity. These features combined indicate that assembly of functionalized subunits will more often result in "dead end structures". Given these observations, it is not likely this statistical re-assembly approach of heteropolymeric apoferritin of equine spleen can be translated towards the introduction of larger substituents such as targeting peptides. For such substituents, a solution may lie in the initial use of small bi-functional linkers. These substituents can be used to introduce new reactive groups such as (protected) thiols or azides,[43,44] which can be selectively functionalized after the re-assembly process.[45]

Changing towards a more simplified re-assembly platform could also have a positive effect on the results. The Ferritin family has other members beside the mammalian equine spleen ferritin, such as the DNA-binding proteins from starved cells (Dps), or homopolymeric bacteria ferritins (Bfr).[29] While the mammalian ferritin is built up from heavy (H) and light (L) subunits (24 in total), Dps only consist of 12 such subunits,[25] and homopolymeric Bfr is only build up from H subunits (24 in total).[29,46] These latter two ferritin types are less complex in their structure, and thereby may provide a re-assembly process that is more suitable for functionalization.

To validate if Cy3- and Cy5-functionalized subunits were in fact combined on the same capsids, their photophysical interactions were analysed. If Cy3 and Cy5 are on the same molecule, and in close proximity to each other (< 10 nm), Föster Resonance Energy Transfer (FRET) should occur from Cy3 to Cy5.[47] Since ferritins surface area is 452 nm^2 ($4\pi r^2$, with r = 6 nm) and there are 10 ± 2 dyes on average after orthogonal functionalization, each dye has 45.2 nm^2 circle space (assuming they are equally spaced); this results in an r_{dye} of 3.8 nm. This distance should be sufficient to allow for FRET. Indeed Cy3 excitation at 525 nm resulted in two peaks corresponding to Cy3- (570 nm) and Cy5-emission (670 nm). The intensity of the FRET emission decreased with decreasing Cy3:Cy5 ratio (Figure 4, B). Even with Cy5 quantities as low as one Cy5 per ferritin capsid (Cy3:Cy5:non-functionalized = 9.0:1.3:13.7) FRET could still be observed (Figure 4, B).

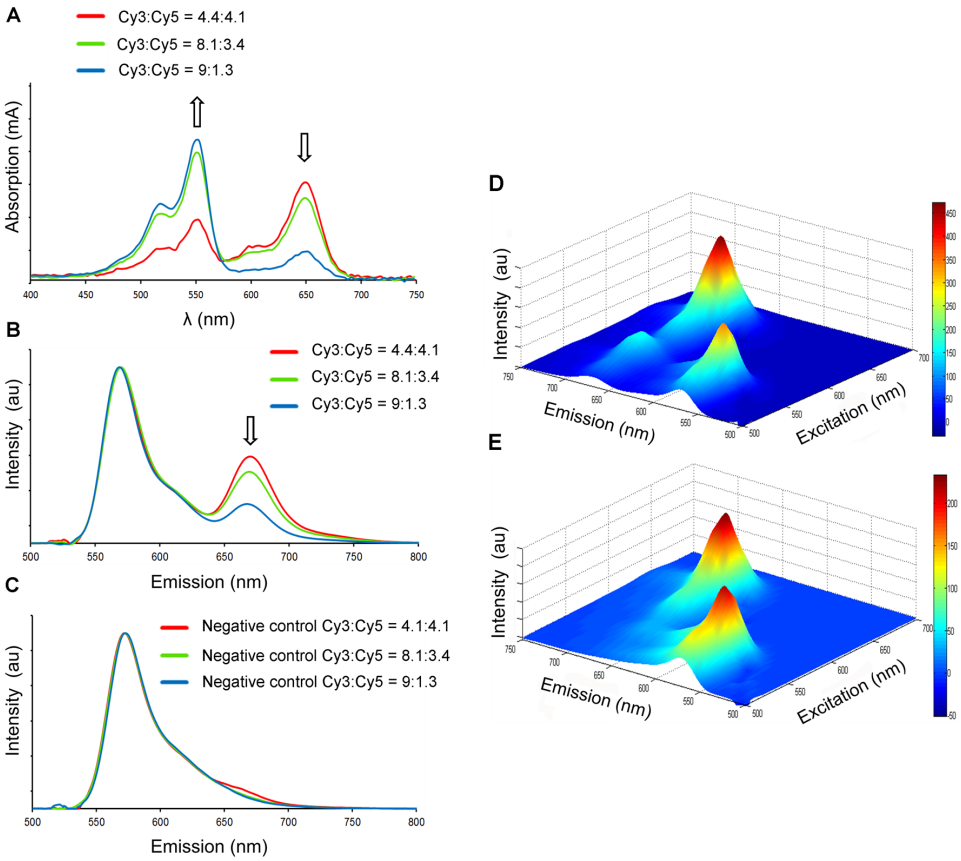

Figure 4. Photophysical measurements of orthogonal functionalized ferritin. **A**) Absorption measurements normalized on ferritin content, arrows indicate the increasing and decreasing signal of Cy3 and Cy5 upon increasing Cy3:Cy5 ratio. **B**) Normalized fluorescence emission spectra after excitation at 525 nm. With increasing Cy3:Cy5 ratio, the FRET signal decreases with the amount of Cy5 dyes. **C**) Control for FRET measurements shown in B; samples contain mixtures of separate Cy3- and Cy5-function-alized ferritin capsids at similar Cy-dye concentrations as the corresponding re-assembled capsids. **D**) 3D fluorescence emission spectrum showing FRET of Cy3:Cy5:non-functionalized = 6.5:6.5:11 functionalized ferritin, excited from 525 to 700 nm. **E**) Control for FRET measurement shown in C; mixture of separate Cy3- and Cy5-functionalized ferritin capsids at similar concentrations as the Cy3:Cy5:non-functionalized = 4.4:4.1:15.5 re-assembled capsids.

To confirm the (FRET) origin of the observed Cy5 emission, mixtures of separate Cy3- and Cy5-functionalized ferritin capsids were measured with similar Cy3 and Cy5 concentrations as the corresponding re-assembled capsids. Other than in the dual-

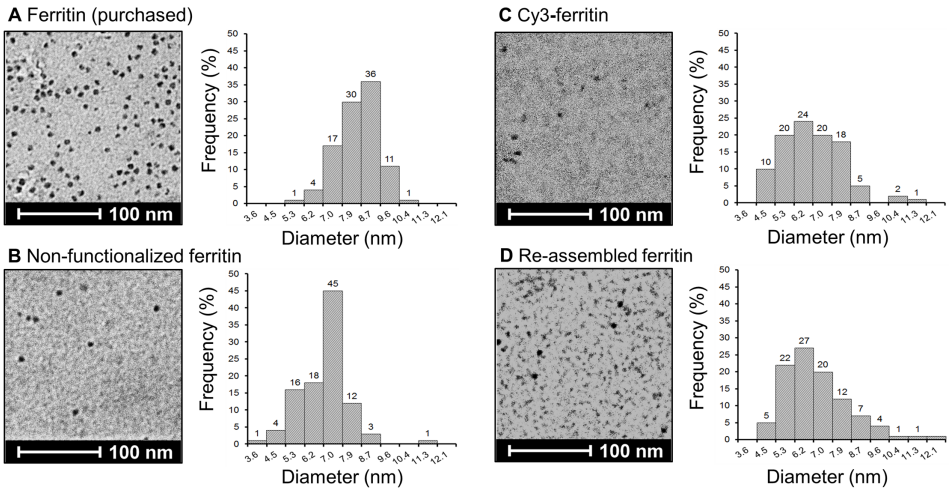

Figure 5. TEM analysis of FeII biomineralization with corresponding size hystograms.of purchased ferritin containing iron and ferritin samples treated with 1000 molar Fe excess to ferritin capsids. **A**) Commercially purchased ferritin, **B**) Non-functionalized ferritin, **C**) Cy3-functionalized ferritin, and **D**) re-assembled multi functionalized ferritin.

functionalized capsids, in these control samples FRET interactions (Cy5 emission peak afterCy3 excitation) could not be observed (Figure 4, C). To further visualize the FRET effect a 3D plot (Figure 4, D) of the excitation and emission spectrum Cy3:Cy5:non-func-tionalized = 4.4:4.1:15.5 was measured together with its negative control (Figure 4, E). The conclusion that Cy3 and Cy5 are indeed located on the same capsid after re-assembly was also underlined by additional SEC measurements (Supporting Information).

Iron Biomineralization by Multi Functionalized Ferritin

The biomineralization properties of ferritin results in the Fe^{II} nucleation into a ferrimagnetic iron core.[48-50] To validate if orthogonally functionalized ferritin capsids are still cap-able of iron mineralization, they were dissolved in an iron-ion rich solution and analysed using TEM. The same was done with non-functionalized (apo) ferritin and Cy3-func-ionalized ferritin. The obtained images were compared to commercially purchased iron bearing ferritin (Figure 5, A). The iron cores are visible in each image (Figure 5) as dark dots, with an average diameter of: 7.8 ± 0.9 nm for purchased ferritin, 6.2 ± 1.0 nm for non-functionalized ferritin, 6.1 ± 1.4 for Cy3-functionalized ferritin, and 6.3 ± 1.5 nm for re-assembled Cy3-, Cy5-functionalized ferritin. The loading method for iron, resulted in

Table 2. ICP-MS results of indicated ferritin samples.

Sample	Ferritin µMol/L[a]	Fe mmol/L[b]	Fe / Ferritin % [c]
Ferritin (purchased)	14.7	3.6	100
Non-functionalized ferritin	13	1.5	48.4
Cy3-ferritin	9.1	0.7	29.7
Re-assembled ferritin	1.9	0.2	50.0

[a] Determined by absorption measurements. [b] Determined by ICP-MS measurements. [c] Iron loading percentage relative to purchased ferritin.

approximately 2 nm smaller sized iron cores compared to the purchased ferritin, with a slightly larger spread in size for the functionalized ferritin capsids (Figure 5, C and D).

According ICP-MS the biomineralisation properties of ferritin are retained by the re-assembled Cy3-, Cy5-functionalized ferritin capsids and seem as efficient as for the non-functionalized ferritin (Table 2). Only the Cy3-func-tionalized ferritin yielded slightly lower percentage of Fe^{III} particles per capsid. Apparently, the higher quantity of Cy-dyes conjugated to the capsid, 16 instead of 8.5 as for the re-assembled ferritin, reduced the inwards diffusion of iron. That the biomineralization of iron inside the re-assembled Cy3-, Cy5-functionalized ferritin capsids was as efficient as for non-functionalized ferritin capsids was further con-firmed by fluorescence measurements (Supporting Information); by increasing iron concentration within the capsids the fluorescence quenching of the proteins (manly tyrosine) is quenched.[51-53]

In theory, the re-assembled ferritin capsids might be one subunit short, as discussed above.[41] If this occurs, however, it does not seem to influence the iron-mineralization process. As a result, the described orthogonal functionalization technique seems compatible with iron loading and could be an additional tool in the future development of MRI contrast agents.

CONCLUSIONS

With these studies we have shown that ferritin can act as supramolecular basis for the controlled generation of orthogonally functionalized ferritin bio-nanoparticles that may find and application in e.g. MRI imaging. This said attaching relatively small dye substituents on the protein subunits already had a negative influence on the self-assembly process.

Acknowledgments

The research leading to these results has received funding from the European Research Council (ERC) under the European Union's Seventh Framework Programme FP7/2007-2013 (grant agreement number 2012-306890), from the NWO nano-Grant (STW 11435), and from the Netherlands Organisation for Scientific Research (NWO) (STW BGT 11272).

REFERENCES

1. N. F. Steinmetz; D. J. Evans, Utilisation of plant viruses in bionanotechnology. *Org. Biomol. Chem.* **2007,** *5* (18), 2891-2902.
2. L. A. Lee; H. G. Nguyen; Q. Wang, Altering the landscape of viruses and bionanoparticles. *Org. Biomol. Chem.* **2011,** *9* (18), 6189-6195.
3. M. G. Mateu, Assembly, stability and dynamics of virus capsids. *Arch. Biochem. Biophys.* **2013,** *531* (1-2), 65-79.
4. Z. Heger; S. Skalickova; O. Zitka, et al., Apoferritin applications in nanomedicine. *Nanomedicine* **2014,** *9*, 2233-2245.
5. H. N. Munro; M. C. Lincer, Physiological Reviews. *Am. Phy.s Soc.* **1978,** *58* (2), 317 - 396.
6. N. J. Sanghamitra; T. Ueno, Expanding coordination chemistry from protein to protein assembly. *Chem. Commun.* **2013,** *49*, 4114-4126.
7. Z. Zhen; W. Tang; Y.-j. Chuang, et al., Tumor Vasculature Targeted Photodynamic Therapy for Enhanced Delivery of Nanoparticles. *ACS Nano* **2014,** (6), 6004-6013.
8. Q. A. Pankhurst; C. J.; S. K. Jones, et al., Applications of magnetic nanoparticles in biomedicine. *J. Phys. D: Appl. Phys.* **2003,** *36*, R167-R181.
9. J. F. Hainfield, Uranium-loaded apoferritin with antibodies attached: Molecular design for uranium neutron-capture Therapy. *Med. Sci.* **1992,** *89*, 11064-11068.
10. Z. Yang; X. Wang; H. Diao, et al., Encapsulation of platinum anticancer drugs by apoferritin. *Chem. Commun. (Camb)* **2007,** *33* (33), 3453-3455.
11. M. Uchida; M. L. Flenniken; M. Allen, et al., Targeting of Cancer Cells with ferrimagnetic Feritin Cage Nanoparticles. *J. Am. Chem. Soc.* **2006,** *128*, 16626-16633.
12. C. Cao; X. Wang; Y. Cai, et al., Targeted in vivo imaging of microscopic tumors with ferritin-based nanoprobes across biological barriers. *Adv. Mater.* **2014,** *26* (16), 2566-2571.
13. K. Fan; C. Cao; Y. Pan, et al., Magnetoferritin nanoparticles for targeting and visualizing tumour tissues. *Nat. Nanotechnol.* **2012,** *7* (7), 459-464.
14. Z. Zhen; W. Tang; T. Todd, et al., Ferritins as nanoplatforms for imaging and drug delivery. *Expert. Opin. Drug. Deliv.* **2014,** *11* (12), 1913-1922.
15. D. Resnick, Modeling of the magnetic behavior of γ-Fe[sub 2]O[sub 3] nanoparticles mineralized in ferritin. *J. Appl. Physi.* **2004,** *95* (11), 7127.
16. E. Valero; S. Fiorini; S. Tambalo, et al., In vivo long-term magnetic resonance imaging activity of ferritin-based magnetic nanoparticles versus a standard contrast agent. *J. Med. Chem.* **2014,** *57* (13), 5686-5692.

17. B. Cohen; H. Dafni; G. Meir, et al., Ferritin as an endogenous MRI reporter for noninvasive imaging of gene expression in C6 glioma tumors. *Neoplasia* **2005,** *7* (2), 109-117.
18. W. F. Rurup; J. Snijder; M. S. T. Koay, et al., Self-sorting of foreign proteins in a bacterial nanocompartment. *J. Am. Chem. Soc.* **2014,** *136* (10), 3828-3832.
19. H. Zope; F. Versluis; A. Ordas, et al., Om votrp amd om vivo supramolecular modification of biomembranes using a lipidated coiled-coil motif. *Angew. Chem. Int. Ed.* **2013,** (52), 14247-14251.
20. J. M. Pollino; K. P. Nair; L. P. Stubbs, et al., Cross-linked and functionalized 'universal polymer backbones' via simple, rapid, and orthogonal multi-site self-assembly. *Tetrahedron* **2004,** *60* (34), 7205-7215.
21. L. Brunsveld; B. J. B. Folmer; E. W. Meijer, et al., Supramolecular Polymers. *Chem. Rev.* **2001,** *101*, 4071-4097.
22. X. Yan; S. Li; J. B. Pollock, et al., Supramolecular polymers with tunable topologies via hierarchical coordination-driven self-assembly and hydrogen bonding interfaces. *Proc. Natl. Acad. Sci. U S A* **2013,** *110* (39), 15585-15590.
23. P. Besenius; Y. Goedegebure; M. Driesse, et al., Peptide functionalised discotic amphiphiles and their self-assembly into supramolecular nanofibres. *Soft matter* **2011,** (7), 7980-7983.
24. X. Lin; J. Xie; L. Zhu, et al., Hybrid ferritin nanoparticles as activatable probes for tumor imaging. *Angew. Chem. Int. Ed.* **2011,** (7), 1569-1572.
25. S. Kang; L. M. Oltrogge; C. C. Broomell, et al., Controlled Assembly of Bifunctional Chimeric PRotein Cages and Composition Analysis Using Noncovalent Mass Spectrometry. *J. Am. Chem. Soc* **2008,** *130*, 16527-16529.
26. E. Gillitzer; P. Suci; M. Young, et al., Controlled ligand display on a symmetrical protein-cage architecture through mixed assembly. *Small* **2006,** (8), 962-966.
27. M. T. Smith; A. K. Hawes; B. C. Bundy, Reengineering viruses and virus-like particles through chemical functionalization strategies. *Curr. Opin. Biotechnol.* **2013,** *24* (4), 620-626.
28. N. Stephanopoulos; M. B. Francis, Choosing an effective protein bioconjugation strategy. *Nat. Chem. Biol.* **2011,** *7* (12), 876-884.
29. Y. Zhang; B. P. Orner, Self-assembly in the ferritin nano-cage protein superfamily. *Int. J. Mol. Sci.* **2011,** *12* (8), 5406-5421.
30. S. Aime; L. Frullano; S. G. Crich, Compartmentalization of a Gadolinium Complex in the Apoferritin Cavity: A Route To Obtain High Relaxivity Contrast Agents for Magnetic

Resonance Imaging. *Angew. Chem. Int. Ed.* **2002,** *41*, 1017-1019.

31. J. C. Cutrin; S. G. Crich; D. Burghelea, et al., Curcumin/Gd loaded apoferritin: a novel "theranostic" agent to prevent hepatocellular damage in toxic induced acute hepatitis. *Mol. Pharm.* **2013,** *10* (5), 2079-2085.
32. L. Wang; J. Fan; X. Qiao, et al., Novel asymmetric Cy5 dyes: Synthesis, photostabilities and high sensitivity in protein fluorescence labeling. *J. Photochem. Photobiol. A: Chem.* **2010,** *210* (2-3), 168-172.
33. S. stefanini; S. Cavallo; B. Montagnini, et al., Incorporation of iron by the unusual dodecameric ferritin from Listeria innocua. *Biochem. J.* **1999,** *338*, 71-75.
34. S. G. Crich; B. Bussolati; L. Tei, et al., Magnetic resonance visualization of tumor angiogenesis by targeting neural cell adhesion molecules with the highly sensitive gadolinium-loaded apoferritin probe. *Cancer Res.* **2006,** *66* (18), 9196-9201.
35. Silvio Aime; Luca Frullano; S. G. Crich, Compartmentalization of a Gadolinium Complex in the Apoferritin Cavity: A Route To Obtain High Relaxivity Contrast Agents for Magnetic Resonance Imaging**. *Angew. Chem. Int. Ed.* **2002,** *41*, 1017 - 1019.
36. B. Webb; J. Frame; Z. Zhao, et al., Molecular Entrapment of Small Molecules within the Interior of Horse Spleen Ferritin. *Arch. Biochem. Biophys.* **1994,** *309*, 178-183.
37. M. T. Klem; D. a. Resnick; K. Gilmore, et al., Synthetic control over magnetic moment and exchange bias in all-oxide materials encapsulated within a spherical protein cage. *J. Am. Chem. Soc.* **2007,** *129* (1), 197-201
38. E. C. Theil, Ferritin: Structure, gene, regulation, and cellular function in animals, plants, and microorganisms. *Ann. Rev. Biochem.* **1987,** *56*, 289-315.
39. C. Bernacchioni; V. Ghini; C. Pozzi, et al., Loop electrostatics modulates the intersubunit interactions in ferritin. *ACS Chem. Biol.* **2014,** *9* (11), 2517-2525.
40. D. J. Huard; K. M. Kane; F. A. Tezcan, Re-engineering protein interfaces yields copper-inducible ferritin cage assembly. *Nat. Chem. Biol.* **2013,** *9* (3), 169-176.
41. M. Kim; Y. Rho; K. S. Jin, et al., pH-dependent structures of ferritin and apoferritin in solution: disassembly and reassembly. *Biomacromolecules* **2011,** *12* (5), 1629-1640.
42. M. Gerl; R. Jaenicke, Mechanism of the self-assembly of apoferritin from horse spleen. *Eur. Biophys. J.* **1978,** *15*, 103-109.
43. Q. Zeng; T. Li; B. Cash, et al., Chemoselective derivatization of a bionanoparticle by click reaction and ATRP reaction. *Chem. Commun. (Camb)* **2007,** *14* (14), 1453-1555.
44. N. F. Steinmetz; D. J. Evans; G. P. Lomonossoff, Chemical introduction of reactive thiols into a viral nanoscaffold: a method that avoids virus aggregation. *Chembiochem : a European journal of chemical biology* **2007,** *8* (10), 1131-1136.

45. L. I. Willems; H. S. Overkleeft; S. I. Kasteren, Current Developments in Activity-Based Protein Profiling. *Bioconjugate Chem.* **2014,** (25), 1181-1191.
46. M. Liang; K. Fan; M. Zhou, et al., H-ferritin-nanocaged doxorubicin nanoparticles specifically target and kill tumors with a single-dose injection. *Proceedings of the National Academy of Sciences of the United States of America* **2014,** *111* (41), 14900-14905
47. S. Lee; J. Lee; S. Hohng, Single-Molecule Three-Color FRET with Both Negligible Spectral Overlap and Long Observation Time. *PLoS ONE* **2010,** *5* (8), 12270-12279.
48. M. T. Klem; M. Young; T. Douglas, Biomimetic magnetic nanoparticles. *Mater. Today* **2005,** *8* (9), 28-37.
49. N. Chasteen; P. Harrison, Mineralization in ferritin: an efficient means of iron storage. *J. Struct. biol.* **1999,** *126*, 182-194.
50. M. Allen; D. Willits; J. Mosolf, et al., Protein Cage Constrained Synthesis of Ferrimagnetic Iron Oxide Nanoparticles. *Adv. Mater.* **2002,** *14*, 1562-1565.
51. A. B. T. Ghisaidoobe; S. J. Chung, Intrinsic Tryptophan FLuorescence in the Detection and Analysis of Proteins: A Focus on Forster Resonance Energy Transfer Techniques. *Int. J. Mol. Sci.* **2014,** *15* (15), 22518-22538.
52. F. Bou-Abdallah; P. Santambrogio; S. Levi, et al., Unique iron binding and oxidation properties of human mitochondrial ferritin: a comparative analysis with Human H-chain ferritin. *J. Mol. Biol.* **2005,** *347* (3), 543-554.
53. K. Orino; T. Miura; S. Muto, et al., Sequence analysis of canine and equine ferritin H and L subunit cDNAs. *DNA Sequence* **2005,** *16* (1), 58-64.

SUPPORTING INFORMATION CHAPTER 5

Orthogonal Functionalization of Ferritin via Supramolecular Re-Assembly

RESULTS

SEC of multi functionalized re-assembled ferritin

To support the conclusion from the FRET results that Cy3- and Cy5-modified subunits are located on the same ferritin capsid after re-assembly, additional SEC measurements were performed. In these experiments, Uv absorbance at 550 nm and 650 nm was measured, to detect the Cy3- and Cy5-dyes conjugated to the capsids (Figure S1). As negative control for the duo-functionalized ferritin capsids, a mixture of separately functionalized Cy3- and Cy5-ferritin was prepared with the same Cy3 and Cy5 concentration as the re-assembled sample with ratio Cy3:Cy5:non-functionalized = 4.4 : 4.1 : 15.5. Although less conclusive then the FRET data, a difference in the SEC graph between the two samples is visible. For the duo-functionalized ferritin capsids, the Cy3 and Cy5 absorbance signal elute exactly at the same time and form one peak. In contrast, the sample containing the mixture of Cy3- and Cy5-ferritin capsids shows a Cy5 absorbance peak that is slightly shifted in comparison with the Cy3 absorbance peak, resulting in two distinguishable elution peaks. Although this data is not conclusive on its own, together with the FRET data it does support the conclusion that after re-assembly the Cy3- and Cy5-subunits are located within the same ferritin capsid.

Fluorescence of the variable functionalized ferritin capsids

When apoferritin is excited at 270 nm, the proteins emit light between 300 and 400 nm with a maximum at 310 nm (Figure S2), this fluorescence originates from the tyrosine and tryptophan amino acids.[1] With increasing iron concentration within the ferritin capsids the fluorescence of the proteins (mainly tyrosine)[1-2] is quenched. Thereby the amount of quenching is an indication of the number of iron inside.

The decrease in fluorescent signal with increasing Fe^{iii} / capsid is depicted in Figure S2A, where the emission spectra apoferritin and apoferritin treated with 400-, 600-, 800- and 1000 molar excess of iron to ferritin capsids are plotted. Figure S2B shows the fluorescent signal of apoferritin, purchased ferritin containing iron, non-functionalized ferritin, ferritin-Cy3 and re-assembled ferritin of which the latter three were also treated with 1000 molar excess of iron.

The data shows that Cy3-funcitonalized ferritin contains the least amount of iron and that purchased ferritin contains the most, since its fluorescence signal at 340 nm (tryptophan) is also lowered compared to non-functionalized ferritin. The re-assembled ferritin and non-functionalized contain comparable amounts, with non-functionalized ferritin containing slightly more according the 340 nm peak.

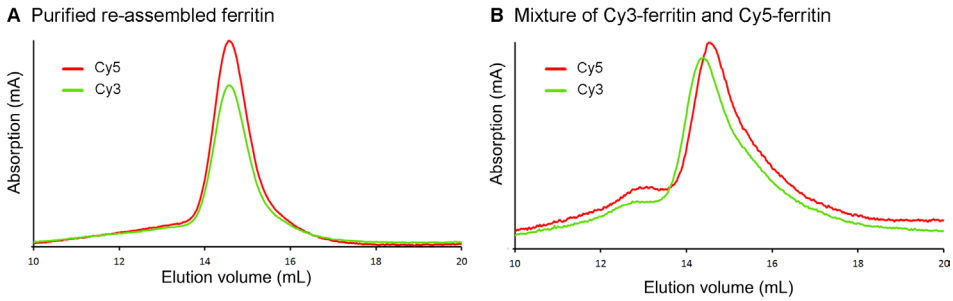

Figure S1. SEC of Cy3-, and Cy5-functionalized ferritin (**A**) and a mixture of separately functionalized Cy3-ferritin and Cy5-ferritin (**B**). With red: the absorption signal of Cy5 (650 nm) and green: the absorption signal of Cy3 (550 nm) of the corresponding sample, both absorbance signals were measured simultaneously.

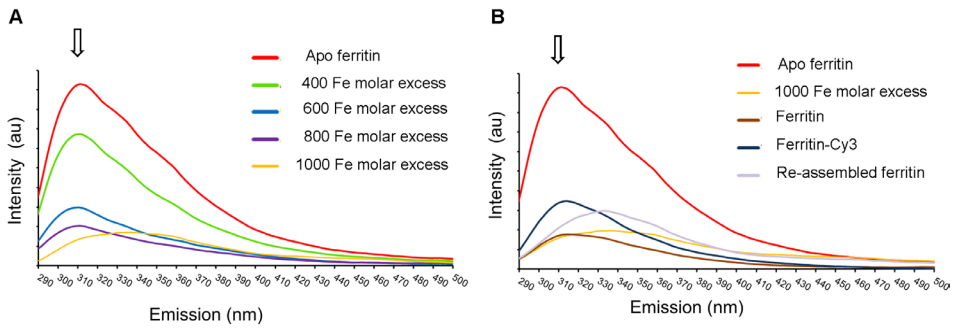

Figure S2. Emission spectra of ferritin capsids after excitation at 270 nm with ferritin capsids concentration set at 0.05 absorbance. **A**) Ferritin capsids treated with increasing molar excess of iron to ferritin capsid. **B**) Non-functionalized, Cy3-functionalized and re-assembled ferritin after treatment with 1000 molar excess of iron to ferritin capsids, purchased ferritin and apoferritin are shown for comparison.

REFERENCES

1. A. B. T. Ghisaidoobe; S. J. Chung, Intrinsic Tryptophan FLuorescence in the Detection and Analysis of Proteins: A Focus on Forster Resonance Energy Transfer Techniques. *Int. J. Mol. Sci.* **2014,** *15* (15), 22518-22538.
2. K. Orino; T. Miura; S. Muto, et al., Sequence analysis of canine and equine ferritin H and L subunit cDNAs. *DNA Sequence* **2005,** *16* (1), 58-64.

Adapted from: Spa SJ, Hensbergen AW, van der Wal S, Kuil J, van Leeuwen FWB.
Dyes and Pigments 2018;152:19-28

and

Spa SJ, Hensbergen AW, van der Wal S, Kuil J, van Leeuwen FWB.
Data Brief 2019;22:50-55